nature astronomy

LETTERS

PUBLISHED: 17 JULY 2017 | VOLUME: 1 | ARTICLE NUMBER: 0179

# A Martian origin for the Mars Trojan asteroids

D. Polishook[1]*, S. A. Jacobson[2,3], A. Morbidelli[3] and O. Aharonson[1]

**Seven of the nine known Mars Trojan asteroids belong to an orbital cluster[1,2] named after its largest member, (5261) Eureka. Eureka is probably the progenitor of the whole cluster, which formed at least 1 Gyr ago[3]. It has been suggested[3] that the thermal YORP (Yarkovsky–O'Keefe–Radzievskii–Paddack) effect spun up Eureka, resulting in fragments being ejected by the rotational-fission mechanism. Eureka's spectrum exhibits a broad and deep absorption band around 1 μm, indicating an olivine-rich composition[4]. Here we show evidence that the Trojan Eureka cluster progenitor could have originated as impact debris excavated from the Martian mantle. We present new near-infrared observations of two Trojans ((311999) 2007 $NS_2$ and (385250) 2001 $DH_{47}$) and find that both exhibit an olivine-rich reflectance spectrum similar to Eureka's. These measurements confirm that the progenitor of the cluster has an achondritic composition[4]. Olivine-rich reflectance spectra are rare amongst asteroids[5] but are seen around the largest basins on Mars[6]. They are also consistent with some Martian meteorites (for example, Chassigny[7]) and with the material comprising much of the Martian mantle[8,9]. Using numerical simulations, we show that the Mars Trojans are more likely to be impact ejecta from Mars than captured olivine-rich asteroids transported from the main belt. This result directly links specific asteroids to debris from the forming planets.**

We observed the second and third in the size-ordered list of (5261) Eureka cluster members: (311999) 2007 $NS_2$ and (385250) 2001 $DH_{47}$, with diameters of 0.7 ± 0.2 and 0.5 ± 0.1 km, respectively (see Supplementary Information for details). Observations were conducted in February 2016 at the NASA Infrared Telescope Facility with the (Spectropolarimeter for Planetary Exploration (SPEX) instrument at a wavelength range of 0.8 to 2.5 μm (see Methods for details).

The reflectance spectra of both 2007 $NS_2$ and 2001 $DH_{47}$ match one another (Fig. 1a). With a broad absorption band around 1 μm, they resemble the olivine-rich A-type of the Bus–DeMeo classification. In addition, the lack of an absorption band at 2 μm reflects the lack of iron-bearing pyroxene. These measurements confirm the results of recent ground-based observations obtained independently with the XSHOOTER spectrograph on the Very Large Telescope[10]. Eureka was classified as Sa-type[11], a subclass of the olivine-rich A-type. Using a radiative-transfer, composition-mixing model (the Shkuratov model[12,13]), we characterized the asteroid reflectance spectra and found that Eureka, 2007 $NS_2$ and 2001 $DH_{47}$ have about 90% ± 10% olivine at the surface.

The observed width of the 1 μm absorption band differs significantly from those of S-complex asteroids (S-, Sq-, Q-types, and so on; Fig. 1a), refuting any spectral connection with these common asteroid types. Similarly, we rule out a match with the flat reflectance spectra of C- and X-complex asteroids. An unbiased census of the main belt shows that only 0.4% of the mass of the main-belt asteroids are the olivine-rich A-types[5]. This makes the similarity between the reflectance spectra of Eureka, 2007 $NS_2$ and 2001 $DH_{47}$ even more striking. Therefore, we conclude that it is likely that the three observed Trojans share the same progenitor, as suggested by dynamical calculations[3]. Inductively, the other four members of the Eureka cluster are likely to have the same origin and composition. This hypothesis should be tested when they will be available for observations in March–April 2018.

The conclusion that seven of the nine known Mars Trojans might originate from a single olivine-rich progenitor motivates the deeper question of that body's origin and its transport to the fifth Lagrange point of Mars. Given the rarity of olivine-rich asteroids, if the Mars Trojan population were drawn from a background population of asteroids sourced from the main belt, then one would expect more than 200 similarly sized Mars Trojans of more common compositions (that is, S-complex, C-complex and X-complex), rather than just the other two observed Mars Trojans (one S-complex and one X-complex), in addition to the olivine-rich cluster of asteroids.

Instead, we present evidence that the parent body of this cluster, that is, Eureka, originated from Mars itself and was ejected from the planet due to a large impact, perhaps of similar scale to the impact that formed the Borealis Basin. Olivine is predicted to be the most abundant mantle mineral in Mars[8,9], with pyroxene and garnet as minor constituents. In Fig. 1b we compare the reflectance spectra of the Mars Trojans with those of Shergottites, Nakhlites and Chassignites meteorites[7] and measurements of the Martian surface at Nili Fossae[14] indicating compositions containing more than 20% olivine[6], which were collected by the Compact Reconnaissance Imaging Spectrometer for Mars (CRISM). However, can impact ejecta from Mars be dynamically transferred into a Mars Trojan orbit?

No impact ejecta from Mars can be captured immediately into a Mars Trojan orbit. This is most easily understood by approximating the Sun–Mars-ejecta dynamics with the circular restricted three-body problem[15]. A significant change in the Jacobi constant of the ejected body is required to transfer from an orbit that intersects the planet to a co-orbital 'tadpole' orbit about one of the Lagrange points.

We propose instead that it is the orbit of Mars that 'jumps', changing its orbital energy as a reaction to gravitational scattering events from other planetary embryos during the final stages of planet formation. Martian semi-major axis jumps occur throughout planet formation[16]. If ejecta are present within a co-orbital width (defined to be the maximal width of a tadpole orbit[15]) of the new semi-major axis of Mars, then they may be captured into a Trojan orbit. Semi-major axis jumps of Mars occurred only during the era of planet formation because only then did Mars have close encounters with large enough planetary embryos, and it is only the last semi-major axis jump of Mars that could capture the current Mars Trojans, because any subsequent jump would free any captured previously.

Here, we demonstrate that Martian impact ejecta are not immediately removed from the Mars-crossing region and these ejecta can

[1]Department of Earth and Planetary Sciences, Weizmann Institute of Science, Rehovot 7610001, Israel. [2]Bayerisches Geoinstitut, Universtat Bayreuth, 95440 Bayreuth, Germany. [3]Laboratoire Lagrange, Observatoire de la Cote d'Azur, 06304 Nice, France. *e-mail: david.polishook@weizmann.ac.il

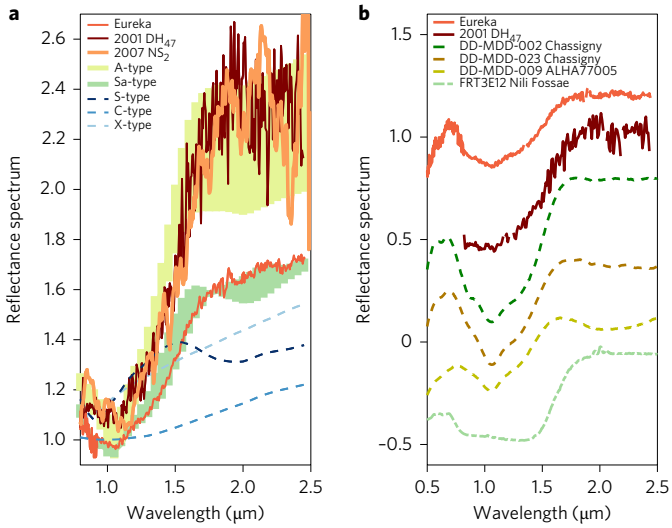


**Figure 1 | Reflectance spectra comparison. a**, The reflectance spectra of the Mars Trojans (5261) Eureka, (311999) 2007 $NS_2$ and (385250) 2001 $DH_{47}$ (dark orange, light orange and brown lines, respectively) compared with the rare olivine-rich A- and Sa-types (light and dark green areas, respectively) and the common S-, C- and X-types classification (blue dashed lines) in the Bus–DeMeo taxonomy[11]. The spectrum of Eureka was reported in ref. 4. The spectrum of 2007 $NS_2$ has been smoothed by a running window of width 0.075 μm. **b**, Comparison of the continuum-removed reflectance spectra of Eureka and 2001 $DH_{47}$ (orange and brown lines, respectively) with three samples from the olivine-rich Martian meteorites Chassigny and Allan Hills (green, light brown and tan dashed lines, respectively). (Spectra are from RELAB: http://www.planetary.brown.edu/relabdocs/relab_related_data.htm.) The 1 μm absorption band of both asteroids lies within the spectral range of the three meteoritic samples, whereas none of the presented reflectance spectra has a band at 2 μm. An atmospheric-corrected reflectance spectrum from the Nili Fossae region on Mars[14], measured by CRISM, also presents an olivine-rich material (light green dotted line). Each spectrum has been shifted vertically for clarity. The reflectance spectrum of 2007 $NS_2$ is omitted because it is similar to that of 2001 $DH_{47}$ but with a lower signal-to-noise ratio. The uncertainty of the measurements (Trojans, meteorites, Mars) is of the order of the spectral scattering. The standard deviation of the S-, C- and X-types classification increases with wavelength and ranges from 3% to 15%.

be captured around a Lagrange point during the final semi-major axis jump of Mars. First, we simulate the dispersal of post-impact debris from about Mars until most of the ejecta have been dispersed, that is, 200 Myr (see Methods). As shown in Fig. 2a, only a small fraction (about 3% at most) of all ejecta have eccentricities ($e$) and inclinations ($i$) within the zone ($e < 0.2$ and $10° + 20° (e / 0.25) < i < 30°$) identified as stable in the co-orbital region[17]. This stability zone is defined by secular resonances, which may have been different during the era of planet formation, but using the current secular structure is the simplest assumption[18]. These ejecta are distributed in orbital distance (semi-major axis, $a$) away from Mars according to the contours shown in Fig. 2b. Initially, the ejecta are placed on low inclination orbits similar to Mars that are not stable. Subsequent planetary encounters over the next 10 Myr increase the inclinations of these bodies, resulting in increasing number of bodies in the stability zone. Thus, we can calculate the probability for an ejected body to be within both the $e$ and $i$ stability zone and within a co-orbital distance (Hill radius) from Mars's location after its final jump in semi-major axis from these contours.

Second, using 61 previously published simulations of terrestrial planet formation[19,20], we determine what fraction of ejecta is placed within the co-orbital radius of a Mars-like planet after its final semi-major axis jump. From each simulation, we assess the time of each impact on the Mars-like planet as well as its semi-major axis at that time, and determine the time of the final semi-major axis jump of the Mars-like planet and its final semi-major axis. As shown in Fig. 3a, the change in the semi-major axis of Mars generally increases as the elapsed time between the impact and the final semi-major axis jump increases. Using these times and distances as input, we determine the odds that ejecta will be captured in each simulation using the probability calculator described above.

Finally, we convert these probabilities into production rates of Mars Trojans. We note that when Mars obtains its final semi-major axis, it is not guaranteed that an ejected body with the correct $a$, $e$ and $i$ will have the correct Jacobi constant. Indeed, given a random orbit in the co-orbital space and within the specified $a$, $e$ and $i$ space, only about 57% of all possible orbits will be stable Mars Trojans according to the solution of the circular restricted three-body problem[15]. The production rate of Mars Trojans from a particular impact decreases exponentially as a function of time with a half-life of 40 Myr (Fig. 3b), which is directly related to the exponential loss of ejecta from within the stability zone due to scattering by Mars (Fig. 2a). The exceptions are those impacts that occur within a few Myr of the final semi-major axis jump. Ejecta in these cases are still clustered at semi-major axes near the semi-major axis of Mars at the time of the impact (Fig. 2b). Overall, because ejecta are most efficiently captured in Trojan orbits that occur within 10 Myr of the final semi-major axis jump of Mars, the production rate of Mars Trojans increases with time towards the end of the planet formation epoch (Fig. 3c). However, early impacts can still have high production rates if the semi-major axis of Mars does not change significantly between the time of the debris-generating impact and its location after its final jump.

We estimate the amount of ejecta from the hypothesized basin impact from numerical impact models of the Borealis Basin[21], but we emphasize that Eureka does not need to originate from the Borealis Basin-forming impact itself (see Methods). The size distribution of impact debris is estimated[22] to have a cumulative slope of −2.85, and so the debris size distribution to produce the mass ejected from the Borealis Basin is:

$$N(>D) = \left(\frac{D}{114\ \mathrm{km}}\right)^{-2.85} \quad (1)$$

where $N(>D)$ is the number of asteroids with diameters greater than $D$. The progenitor of Eureka and its cluster was ~2 km in diameter[23]. Therefore, the above size distribution predicts that there should be ~$10^5$ objects of this size or greater ejected from Mars during a Borealis Basin-size impact.

In summary, there is a dynamical pathway for the Eureka cluster progenitor to go from the interior of Mars to a Mars Trojan orbit, and impacts such as the Borealis Basin eject a sufficient number of debris fragments for capture to be an expected outcome. Examining Fig. 3c in detail, we see that the expected number of Mars Trojans is as high as 15 for every $10^5$ pieces of ejecta launched from Mars if the last semi-major axis jump of Mars occurs in the first 10 Myr after the ejecta are launched. If the last semi-major axis jump of Mars occurs later, then the number of expected Mars Trojans from the ejecta cloud decreases.

The high likelihood that a piece of impact ejecta is captured as a Mars Trojan is especially striking when considering how rare A-type asteroids are in the asteroid belt[5] (0.4% mass fraction). The other two Mars Trojans are identified as S-complex and X-complex members, and both are more common types in the main belt[5] (mass fractions of 8.4% and 14.3%, respectively). Thus, the likelihood of randomly drawing just the two Mars Trojans of more common types from a main-belt-like distribution of compositions is two orders of magnitude greater than the likelihood of drawing all

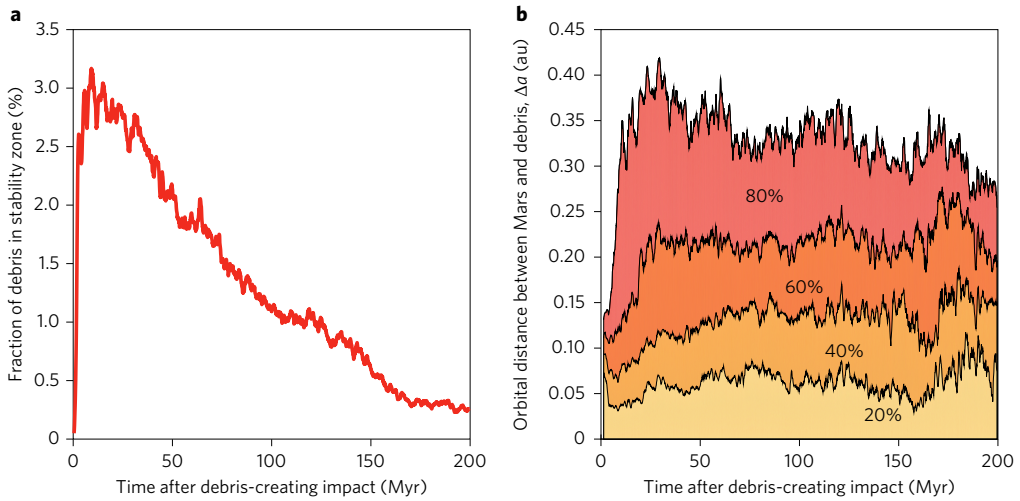


**Figure 2 | Impact ejecta dispersal. a**, The surviving fraction of the Martian debris averaged over all simulations as a function of time after the debris-creating impact that are within the eccentricity $e$ and inclination $i$ ranges $e < 0.2$ and $[10° + 20°(e / 0.25)] < i < 30°$, corresponding to the co-orbital stability zone[17] and any orbital distance from Mars. **b**, Contours that contain a constant fraction of the impact debris cloud in the stability zone between the orbital distance (that is, difference in semi-major axis, $\Delta a$) on the ordinate and Mars as a function of time after the impact. In both panels, the curves are 1 Myr moving averages combining the results from all simulations. The contours in **b** contain 20%, 40%, 60% and 80% of surviving debris from bottom to top.

three Mars Trojans (that is, including the A-type Eureka progenitor) from the same distribution.

An objection may be raised that, although the A-types are rare overall, they do make up about 7% of the mass of the Hungarias—a nearby asteroid population whose membership can interchange with the Mars-crossing population[24]. However, the source of the A-types in the Hungarias is not clear. There is no evidence of an A-type family amongst the Hungarias[5], and because dynamical transport is independent of composition, it is unlikely that A-type asteroids could be preferentially sourced from the main belt where they are much rarer. Indeed, it is possible that the A-type Hungarias originate from the same Martian ejecta as the A-types in the Mars Trojan population. To test this hypothesis, we determine that 7 out of 5,000 simulated Martian ejecta end up on stable orbits in the Hungaria region ($1.75 < a < 2.0$ au, $e < 0.2$ and $15° < i < 40°$), which is an efficiency of $0.14 \pm 0.06\%$ with an uncertainty estimated from Poisson statistics. Given that a Borealis Basin-size impact generates approximately one Mars Trojan, this impact would deliver about $4.5 \times 10^{17}$ kg of A-type material to the Hungaria region or about 12 times what is observed there today[5]. This implies a dynamical depletion half-life of the Hungaria asteroids of about 1.3 Gyr, which is broadly consistent with various numerical modelling estimates from the literature[25,26].

We have shown that the Eureka cluster asteroids are consistent with being from the plutonic rock of Mars. While impact debris creation has been discussed as an important process during planet formation[27], until now there has been no direct evidence that it has occurred. The Martian meteorites testify that ejecta can escape their parent body, but these ejecta are associated with much later impacts[28]. The Eureka cluster is the lowest delta-V target for a Mars mantle sample-return mission, making it a potential target for space exploration. Furthermore, we have shown that impacts on Mars are more likely to seed the Hungarias with olivine-rich material than the asteroid belt. In fact, it is unclear whether any of the observed olivine-rich material amongst the small-body populations is sourced from planetesimals because ejecta are even able to enter the asteroid belt[29].

## Methods

**Observations, reductions and analysis.** We performed near-infrared (0.8–2.5 μm) spectral observations using SPEX, an imager and a spectrograph mounted on the 3 m telescope of the NASA Infrared Telescope Facility. We used a long slit with a 0.8 arcsec width and shifted the objects along it in an A-B-B-A sequence to allow the measurement of the background noise. The observations were limited to low air mass values between 1.0 and 1.6 to reduce chromatic refraction that can change the spectral slope. The exposure time ranged from two to three minutes per image, while the entire sequence lasted for about two hours, including reading-out time. The observational details are listed in the Supplementary Table 1.

The reduction of the raw SPEX images followed standard procedures[11,30]. This included flat field correction, sky subtraction, manual aperture selection, background and trace determination, removal of outliers and a wavelength calibration using arc images. A telluric correction routine was used to model and remove telluric lines. Each spectrum was divided by a standard solar analogue to derive the relative reflectance of the asteroid. We observed two stars from the Landolt Equatorial Standards list (http://www.cfht.hawaii.edu/ObsInfo/Standards/Landolt/) that are extensively used as solar analogues[11], 98–978 and 102–1081. The normalization using both stars gave comparable results.

To compare the reflectance spectra of the Eureka cluster with the spectra of Shergottites, Nakhlites and Chassignites meteorites and that of Nili Fossae[14] (Fig. 1b), we removed the continuum by dividing the asteroids' reflectance spectra in the linear slope that fit to the spectral maxima tail of the asteroid (from 1.8 to 2.5 μm), and normalized the entire spectral set to unity at 1.8 μm (outside the 1 μm band). We do not present band analysis or a modified Gaussian model, because the parameters fitted by these analysis methods are too sensitive to the quality of our measured spectra of 2007 $NS_2$ and 2001 $DH_{47}$.

**Dynamical model.** We demonstrate that Martian impact ejecta are not immediately removed from the Mars-crossing region and that these ejecta can be captured around a Lagrange point during the final semi-major axis jump of Mars. First, using a symplectic N-body method[31] modified to handle close encounters, called SyMBA[32], we simulated the dispersal of post-impact debris from about Mars in its current orbit. In each of 50 simulations, 100 test particles were randomly placed at a Hill radius distance around Mars at a random location in its orbit, with a velocity vector directed away from Mars and magnitude equal to the escape velocity from that distance plus a 1% enhancement for half the particles and a 10% enhancement for the other half. The differences between the two populations disappear within a few Myr. Including all seven other planets on their current orbits, we integrated the system for 200 Myr, when most of the ejecta have been dispersed.

We determine the impact history and semi-major axis jump distances of Mars using Mars-like planets from 61 previously published simulations of terrestrial planet formation[19,20]. All simulations are from the Grand Tack planet formation scenario, which is notable for being able to form a Mars-like planet[16]. The simulated Mars-like planets have semi-major axes exterior of 1 au but interior of 2.5 au and masses of Mars within a factor of two. The impact history is the record of planetesimal impacts on each Mars-like planet, and the semi-major axis jump distance is determined by recording the semi-major axis at the time of each planetesimal impact and the final semi-major axis of Mars. We also recorded the time between each planetesimal impact and the last semi-major axis jump

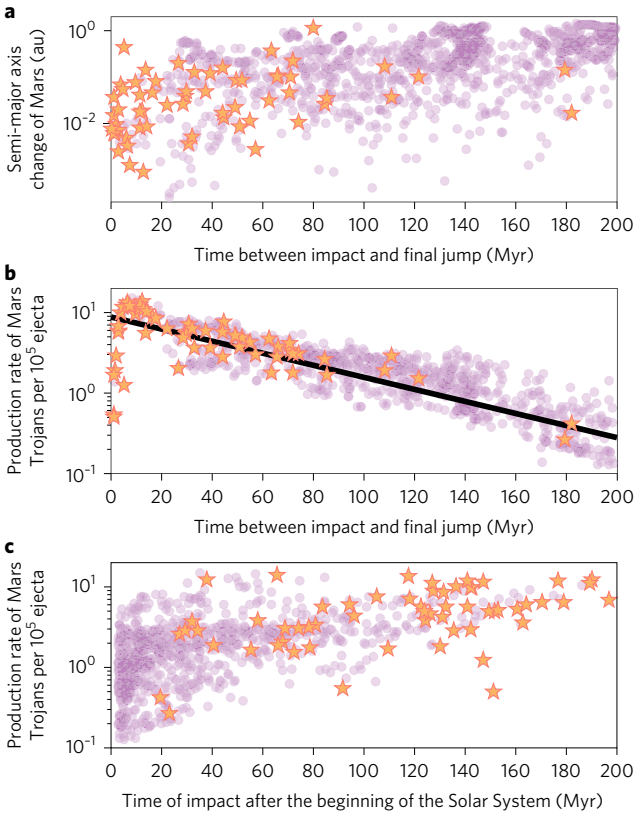


**Figure 3 | Production rate of Mars Trojans.** Symbols represent each planetesimal impact on each Mars-like planet from a suite of terrestrial planet formation simulations: orange stars are the last planetesimal impacts before the final semi-major axis jump of Mars, and purple circles are all previous planetesimal impacts. **a**, The semi-major axis change of each Mars-like planet as a function of the elapsed time between each planetesimal impact on Mars and when Mars makes its final semi-major axis jump. This final jump can be due to the last impact, but it is more often due to a last encounter of Mars with another embryo in the protoplanetary disk. **b**,**c**, The production rate of Mars Trojans for every $10^5$ ejecta launched during the impact. From the size distribution of impact debris (equation (1)) and the combined diameter of the Eureka cluster (~2 km), there should be about $10^5$ objects of this size or greater ejected from a Borealis Basin-size impact on Mars. In **b**, the production rate is shown as a function of time between when the impact occurs and when the planet makes its final semi-major axis jump. In **c**, the production rate is shown as a function of the time of the impact after the beginning of the Solar System. In **b**, an exponential fit to the data with a half-life of about 40 Myr is also shown (black line; $y = 8.8e^{-x/58}$).

of Mars, which occurred when the Mars-like planet last changed its semi-major axis by more than one Hill radius.

**Using the Borealis Basin as an impact reference.** We estimate the amount of ejecta from the hypothesized Borealis Basin impact scenario from numerical impact models to put the needed quantity of ejecta in the context of a recorded basin on Mars, but we emphasize that Eureka does not need to originate from the Borealis Basin-forming impact. In fact, this seems unlikely because the Martian satellites, Phobos and Deimos, do not spectrally match the Eureka cluster progenitor[33] despite arguments that they originated from the Borealis Basin-forming impact on Mars[34]. However, mineralogical diversity amongst the ejecta may be expected because ejecta are likely to include Martian crust and mantle as well as material from the projectile. The moons will probably obtain an average composition of the ejecta that end up in the disk, whereas the Eureka progenitor could be representative of a particular end-member. Currently, there are not enough constraints to determine whether the Borealis Basin-forming event is also the impact that ejected the Eureka cluster progenitor. Early in Martian history, Mars would have been struck by a number of large planetesimals, as evident in simulations of planet formation[20]. However, for much of that history, the Martian lithosphere may have been too warm to record large impact basins even though these impacts would have generated impact debris. Thus, it is not necessary for the Borealis Basin-forming event to be the source of the Mars Trojans. However, the Borealis Basin is a demonstrative example of a sufficiently large impact on Mars.

The Borealis Basin impactor is estimated to be ~0.026 Mars masses[21], and it is modelled to have placed $0.3 \times 10^{-3}$ to $1 \times 10^{-3}$ Mars masses in orbit[34]. Impact energy of the order of $\sim 3 \times 10^{29}$ J is found to result with characteristics closely matching the observed Borealis Basin features[35]. It is also found that with such impact energy and an impact velocity of 6 km s$^{-1}$, the maximum ejection velocities are about 11 km s$^{-1}$ for all impact angles, which is much higher than Mars's escape velocity (~5 km s$^{-1}$). Conservatively, we estimate the escaped mass from the Borealis Basin as $\sim 5 \times 10^{-4}$ Mars masses because, in terrestrial Moon-forming simulations[36], between half and equal to the amount placed in orbit is typically estimated. Because the number of ejecta above a given size scales linearly with the ejected mass, the size of the basin is directly proportional to the likelihood that its ejecta are captured as Mars Trojans.

**Data availability.** The data that support the plots within this paper and other findings of this study are available from the corresponding author upon reasonable request.

Received 10 January 2017; accepted 1 June 2017; published 17 July 2017

## References


1. Christou, A. *et al.* New Martian Trojans and an update on the Eureka cluster. In *European Planetary Science Congress Abstracts* Vol. 9, id. EPSC2014-696 (European Planetary Science Congress, 2014).
2. de la Fuente, C. & de la Fuente, R. Three new stable L5 Mars Trojans. *Mon. Not. R. Astron. Soc.* **432,** L31–L35 (2013).
3. Cuk, M. Christou, A. A. & Hamilton, D. P. Yarkovsky-driven spreading of the Eureka family of Mars Trojans. *Icarus* **252,** 339–346 (2015).
4. Rivkin, A. S. *et al.* Composition of the L5 Mars Trojans: neighbors, not siblings. *Icarus* **192,** 434–441 (2007).
5. DeMeo, F. E. & Carry, B. The taxonomic distribution of asteroids from multi-filter all-sky photometric surveys. *Icarus* **226,** 723–741 (2013).
6. Ehlmann, B. L. & Edwards C. S. Mineralogy of the Martian surface. *Annu. Rev. Earth Planet. Sci.* **42,** 291–315 (2014).
7. McSween, H. Y. SNC meteorites—clues to Martian petrologic evolution? *Rev. Geophys.* **23,** 391–416 (1985).
8. Bertka, C. M. & Fei, Y. Mineralogy of the Martian interior up to core–mantle boundary pressures. *J. Geophys. Res.* **102,** 5251–5264 (1997).
9. Zuber, M. T. The crust and mantle of Mars. *Nature* **412,** 220–227 (2001).
10. Borisov, G. *et al.* The olivine-dominated composition of the Eureka family of Mars Trojan asteroids. *Mon. Not. R. Astron. Soc.* **466,** 489–495 (2017).
11. DeMeo, F. E., Binzel, R. P., Slivan, S. M. & Bus, S. J. An extension of the Bus asteroid taxonomy into the near-infrared. *Icarus* **202,** 160–180 (2009).
12. Shkuratov, Y., Starukhina, L., Hoffmann, H. & Arnold, G. A model of spectral albedo of particulate surfaces: implications for optical properties of the Moon. *Icarus* **137,** 235–246 (1999).
13. Burt, B. J., DeMeo, F. E. & Binzel, R. P. Origin and mineralogy of olivine-dominated near-Earth asteroids. In *American Astronomical Society Meeting Abstracts* Vol. 224, abstr. 321.08 (American Astronomical Society, 2014).
14. Mustard, J. F. *et al.* Composition, morphology, and stratigraphy of Noachian crust around the Isidis basin. *J. Geophys. Res.* **114,** E00D12 (2009).
15. Murray, C. D. & Dermott, S. F. *Solar System Dynamics* (Cambridge Univ. Press, 1999).
16. Scholl, H., Marzari, F. & Tricarico, P. Dynamics of Mars Trojans. *Icarus* **175,** 397–408 (2005).
17. Chambers, J. E. Make more terrestrial planets. *Icarus* **152,** 205–224 (2001).
18. Brasser, R. & Lehto, H. J. The role of secular resonances on trojans of the terrestrial planets. *Mon. Not. R. Astron. Soc.* **334,** 241–247 (2002).
19. Walsh, K. J., Morbidelli, A., Raymond, S. N., O'Brien, D. P. & Mandell, A. M. A low mass for Mars from Jupiter's early gas-driven migration. *Nature* **475,** 206–209 (2011).
20. Jacobson, S. A. & Morbidelli, A. Lunar and terrestrial planet formation in the Grand Tack scenario. *Phil. Trans. R. Soc. A* **372,** 20130174 (2014).
21. Marinova, M. M., Aharonson, O. & Asphaug, E. Mega-impact formation of the Mars hemispheric dichotomy. *Nature* **453,** 1216–1219 (2008).
22. Leinhardt, Z. M. & Stewart, S. T. Collisions between gravity-dominated bodies. I. Outcome regimes and scaling laws. *Astrophys. J.* **745,** 79 (2012).
23. Nugent, C. R. *et al.* NEOWISE reactivation mission year one: preliminary asteroid diameters and albedos. *Astrophys. J.* **814,** 117 (2015).
24. McEachern, F. M., Cuk, M. & Stewart, S. T. Dynamical evolution of the Hungaria asteroids. *Icarus* **210,** 644–654 (2010).
25. Cuk, M. Chronology and sources of lunar impact bombardment. *Icarus* **218,** 69–79 (2012)
26. Bottke, W. F. *et al.* An Archaean heavy bombardment from a destabilized extension of the asteroid belt. *Nature* **485,** 78–81 (2012)

27. Bottke, W. F. *et al.* Dating the Moon-forming impact event with asteroidal meteorites. *Science* **348,** 321–323 (2015).
28. Nyquist, L. E. *et al.* Ages and geologic histories of Martian meteorites. *Space Sci. Rev.* **96,** 105–164 (2001).
29. Jacobson, S. A. *et al.* There's too much mantle material in the asteroid belt. In *47th Lunar and Planetary Science Conference* 1895 (Lunar and Planetary Institute, 2016).
30. Polishook, D. *et al.* Observations of "fresh" and weathered surfaces on asteroid pairs and their implications on the rotational-fission mechanism. *Icarus* **233,** 9–26 (2014).
31. Wisdom, J. & Holman, M. Symplectic maps for the n-body problem. *Astron. J.* **102,** 1528–1538 (1991).
32. Levison, H. F. & Duncan, M. J. Symplectically integrating close encounters with the Sun. *Astron. J.* **120,** 2117–2123 (2000).
33. Rivkin, A. S., Brown, R. H., Trilling, D. E., Bell, J. F. & Plassmann, J. H. Near-infrared spectrophotometry of Phobos and Deimos. *Icarus* **156,** 64–75 (2002).
34. Citron, R. I., Genda, H. & Ida, S. Formation of Phobos and Deimos via a giant impact. *Icarus* **252,** 334–338 (2015).
35. Marinova, M. M., Aharonson, O. & Asphaug, E. Geophysical consequences of planetary-scale impacts into a Mars-like planet. *Icarus* **211,** 960–985 (2011).
36. Canup, R. M. & Asphaug, E. Origin of the Moon in a giant impact near the end of the Earth's formation. *Nature* **412,** 708–712 (2001).

## Acknowledgements

We thank F. DeMeo and B. Burt for their help with spectral analysis of olivine asteroids, and J. Mustard for providing CRISM reflectance spectra of Mars. D.P. is grateful to the Ministry of Science, Technology and Space of the Israeli government for their Ramon fellowship for post-docs. S.A.J. and A.M. were supported by the European Research Council Advanced Grant 'ACCRETE' (contract number 290568). O.A. acknowledges support from the Helen Kimmel Center for Planetary Science, the Minerva Center for Life Under Extreme Planetary Conditions and the I-CORE Program of the Planning and Budgeting Committee of the Council for Higher Education and the Israeli Science Foundation (Center No. 1829/12). Observations for this study were performed in Hawaii. We are most fortunate to have had the opportunity to conduct observations from the Mauna Kea Observatory, and we thank the NASA Infrared Telescope Facility staff for their continuous help.

## Author contributions

D.P. and S.A.J. led the project and wrote the manuscript. D.P. ran the observations, reduction and analysis of the spectral data. S.A.J. wrote the dynamical simulations and analysed their results. All authors participated in the interpretation of the results.

## Additional information

**Supplementary information** is available for this paper.

**Reprints and permissions information** is available at www.nature.com/reprints.

**Correspondence and requests for materials** should be addressed to D.P.

**How to cite this article:** Polishook, D., Jacobson, S. A., Morbidelli, A. & Aharonson, O. A Martian origin for the Mars Trojan asteroids. *Nat. Astron.* **1,** 0179 (2017).

**Publisher's note:** Springer Nature remains neutral with regard to jurisdictional claims in published maps and institutional affiliations.

## Competing interests

The authors declare no competing financial interests.